Dual-energy CT revisited: a focused review of clinical use cases

Dual-energy CT revisited: fokussierte Übersicht zur klinischen Anwendung

Authors
Simon Lennartz, David Zopfs, Nils Große Hokamp

Affiliations
Institute for Diagnostic and Interventional Radiology, Faculty of Medicine and University Hospital Cologne, University of Cologne, Cologne, Germany

Keywords
CT, CT-quantitative, diagnostic radiology

received 16.6.2023
accepted 15.10.2023
published online 4.1.2024

Bibliography
Fortschr Röntgenstr 2024; 195: 794–806
DOI 10.1055/a-2203-2945
ISSN 1438-9029

Georg Thieme Verlag KG, Rüdigerstraße 14,
70469 Stuttgart, Germany

Correspondence
PD Dr. Simon Lennartz
Institute for Diagnostic and Interventional Radiology, Faculty of Medicine and University Hospital Cologne, University of Cologne, Kerpener Str. 62, 50937 Cologne, Germany
Simon.Lennartz@uk-koeln.de

ABSTRACT

Background Dual-energy CT (DECT) has been available for more than 15 years and has undergone continuous technical development and refinement. Recently, the first photon-counting CT scanner became clinically available and has the potential to further expand the possibilities of spectral imaging. Numerous studies on DECT have been published since its creation, highlighting the clinical applications of the various reconstructions enabled by DECT.

Methods The aim of this focused review is to succinctly summarize basic principles and available technical concepts of DECT and to discuss established applications relevant to the daily clinical routine.

Results/Conclusion DECT is instrumental for a broad variety of clinical use cases. While some DECT applications can enhance day-to-day clinical practice, others are still subject to broad-scale validation and should therefore be handled with restraint in the clinical routine.

Key Points

1. Virtual monoenergetic images, virtual unenhanced images, and iodine maps are the most well-investigated and relevant dual-energy CT reconstructions for clinical application.
2. Low-keV virtual monoenergetic images (VMIs) yield superior image and iodine contrast, which can be leveraged for improved vessel assessment and lesion conspicuity, or to reduce contrast media or radiation dose. VMIs at intermediate energies can serve as a replacement for conventional grey-scale images. VMIs at high keV enable efficient artifact reduction, which can be further optimized in combination with dedicated metal artifact reduction algorithms.
3. Iodine maps and virtual unenhanced images can improve lesion detection in oncologic imaging and enable lesion assessment in monophasic CT examinations, which may allow a reduction of correlative and follow-up imaging.

Citation Format

- Lennartz S, Zopfs D, Große Hokamp N. Dual-energy CT revisited: a focused review of clinical use cases. Fortschr Röntgenstr 2024; 195: 794–806

ZUSAMMENFASSUNG

Hintergrund Die Dual-Energy-CT (DECT) ist seit mehr als 15 Jahren verfügbar und hat kontinuierliche technische Entwicklungen und Verbesserungen durchlaufen. Kürzlich ist die erste photonenzählende CT klinisch verfügbar gemacht worden, die das Potenzial bietet, die Möglichkeiten der spektralen Bildgebung zu erweitern. Seit ihrer Entstehung wurden zahlreiche Studien zur DECT veröffentlicht, die unterschiedlichste klinische Anwendungen der durch DECT verfügbaren Rekonstruktionen untersuchen.

Methoden Das Ziel dieser fokussierten Übersichtsarbeit ist es, die Grundprinzipien und verfügbaren technischen Konzepte der DECT knapp zusammenzufassen und etablierte Anwendungen zu diskutieren, die für die tägliche klinische Routine relevant sind.

Ergebnisse/Schlussfolgerungen DECT ist ein nützliches Instrument für eine Vielzahl klinischer Anwendungsfälle. Während einige DECT-Anwendungen die klinische Praxis im Alltag verbessern können, bedürfen andere noch der Validierung und sollten daher in der klinischen Routine zurückhaltend eingesetzt werden.

Kernaussagen

1. Virtuell monoenergetische Bilder, virtuell native Bilder und Iodkarten sind die am besten untersuchten und relevantesten Dual-Energy-CT-Rekonstruktionen für klinische Anwendungen.
2. Virtuell monoenergetische Bilder (VMI) niedriger Energien liefern einen verbesserten Bild- und Iodkontrast, was für eine verbesserte Gefäßbewertung und Läsionssichtbarkeit genutzt werden bzw. die Reduktion von Kontrastmittel- oder Strahlendosis ermöglichen kann. VMIs bei mittleren Energien können als Standardrekonstruktionen für die klinische Routine eingesetzt werden. Höherenergetische VMIs ermöglichen eine effiziente Reduktion von Artefakten, die in Kombination mit dedizierten Algorithmen zur Reduktion von Metallartefakten noch weiter optimiert werden kann.
3. Iodkarten und virtuell native Bilder können die Detektion von Läsionen in der onkologischen Bildgebung verbessern und erlauben die Charakterisierung von Läsionen in monophasischen CT-Untersuchungen, was zur Reduktion von ergänzenden bzw. Folgeuntersuchungen genutzt werden kann.

Introduction

The concept of dual-energy computed tomography (DECT) was introduced already in the very early days of CT as it was well known that the attenuation of X-rays is strongly dependent on their energy [1, 2]. Yet, these approaches did not become available in the clinical routine until 2006 when the first dedicated DECT scanner, the Somatom Flash, was introduced by Siemens [3, 4]. This scanner used two tube detector pairs that were set up with a 90° offset to each other and could be used with two different tube voltages (kVp), hence enabling acquisition of absorption characteristics with two different energy spectra. Since then, several other approaches to DECT have been suggested. Besides capabilities to improve the image quality or radiation-dose efficacy of standard (conventional) CT images, all systems allow for the reconstruction of so-called DECT results (sometimes referred to as spectral results), i. e., specific image reconstructions that are enabled by DECT technology and that differ from conventional CT images (see section "DECT Reconstructions Used in Clinical Routine" below). Numerous studies, which highlight the advantages of these reconstructions for different clinical tasks as well as for scientific applications, have been published. Most recently, photon-counting CT (PCCT) became available and it is anticipated to further advance the number of spectral results [5]. The aim of this review is to highlight applications of DECT relevant to clinical routine imaging. Hence, a focus will be set on DECT use cases with a larger body of evidence.

Available dual-energy technologies

Different technological implementations of DECT are commercially available and in clinical use. ▶ **Fig. 1** provides a schematic overview of available DECT concepts and technologies. While different terminologies for the several DECT platforms have been suggested and used in the literature, the Society for Body Computed Tomography and Magnetic Resonance (SBCTMR) recently provided systematic nomenclature to facilitate communication, which will be used throughout this article [6].

To understand the underlying technological concepts of DECT, it is important to acknowledge that X-rays as used in medical imaging refer to a spectrum of photons (or X-ray quanta) of different energies (unit: kiloelectron volt, keV) with the maximum being defined by the tube voltage (kVp). In this spectrum, the energies are not linearly distributed but follow a specific pattern that depends on the X-ray tube materials and other system-inherited characteristics, e. g., filters that are used. Alteration of the X-ray tube voltage will therefore result in a different X-ray spectrum, which is the underlying principle of emission-based DECT. While techniques such as scan-scan and rotate-rotate DECT are available from some vendors, they are severely limited by motion effects and temporal misregistration. The following technical implementations of DECT are commercially available and relevant to routine imaging [7, 8]:

Dual-source DECT (dsDECT): Two tube detector pairs offset by 90° to each other allow for simultaneous acquisition of low- and high-energy attenuation spectra. The reconstructed images from both tubes can be fused to obtain a conventional CT image or used as input for the reconstruction of DECT results.

Rapid kVp switching DECT (rsDECT): Within a single rotation, the tube voltage is changed frequently in a succession of as short as 0.5 ms, enabling acquisition of low- and high-energy attenuation spectra. After angular correction, raw data can be fused to obtain a conventional CT image or be used to reconstruct DECT results.

Twin-beam DECT (tbDECT): A filter made from gold and tin is placed along the Z-axis (out-of-plane) to split the X-ray spectrum into a high-energy component and low-energy component that are read out separately by corresponding detector rows.

Dual-layer DECT (dlDECT): The only available detector-based DECT system includes a horizontally aligned detector that consists of two different scintillator materials with one being more prone to detection of low- and high-energy photons, respectively (from a single X-ray spectrum). Raw data can be processed aggregated or separately to obtain conventional images or DECT results.

Photon-counting CT (PCCT): These systems use a novel detector that allows for direct conversion of photons to energy (without the need for a scintillating layer). The detector, therefore, enables higher resolution of images as well as multi-energy separation. However, due to the novelty of this system, the body of literature is still comparably small.

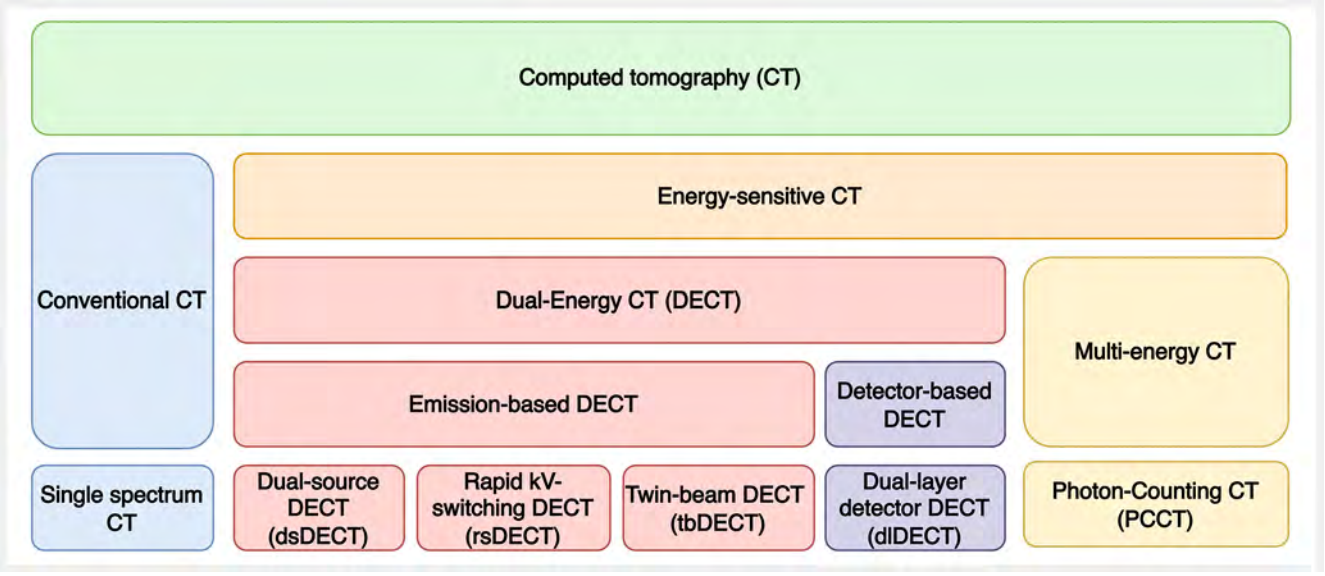

▶ **Fig. 1** Schematic overview of different CT technologies currently available, including conventional, dual-energy, and multi-energy CT

DECT reconstructions used in the clinical routine

While each of the available DECT systems has its own advantages and disadvantages, all systems enable material decomposition for iodine and linear blending of low and high keV X-ray photon data.

Material decomposition exploits the fact that the attenuation of X-rays is dependent on their energy and the composition of the absorbing material. At material decomposition, the dependence of the photoelectric effect as well as Compton scattering, the two main X-ray interactions in the diagnostic energy range, on the atomic number and the physical density of a given material is modeled. This can be achieved by determining the material-specific attenuation coefficient as a linear combination of the attenuation of either two (i. e., two material decomposition) or three (i. e., three material decomposition) base materials in a given voxel [7]. While material decomposition is advantageous in many instances, it is subject to inherent limitations. First, materials with similar absorption characteristics show a "spectral overlap", which may result in erroneous depiction of a confounding material in a material specific map (e. g., calcified structures in iodine maps). This spectral overlap is influenced by different factors such as image noise and the acquisition paradigm. Another limitation of material decomposition is that the presence of a confounding material in a volume of interest may lead to erroneous quantification of the material of interest, since the modeling assumptions are violated [9].

As iodine images selectively depict the iodine-associated component of X-ray attenuation, they allow for absolute quantification of iodine in milligrams per milliliter [10]. The very same information can be subtracted from the conventional image, hence making it possible to obtain virtual unenhanced (VUE) images that closely represent quantitative and qualitative characteristics of a truly unenhanced acquisition [11]. A different way of visualizing iodine content is by reconstructing fused images (similar to well-known PET/CT images): Here, the functional information (i. e., iodine content) is color-coded and superimposed on top of morphological/anatomical reconstructions (see the section on oncology applications). Material decomposition is also available for uric acid as used in the imaging of gout and urinary stones (see the corresponding sections below).

For virtual monoenergetic images (VMIs), linear bending of low- and high-energy information is conducted or extrapolated. VMIs are considered to approximate attenuation characteristics of images acquired with a true monoenergetic X-ray and are therefore indicated by the corresponding, targeted keV level. VMI are available from as low as 40 keV up to 140–200 keV (depending on the DECT technology). Generally, VMIs can be classified according to their energy spectrum as low-energy VMIs (40–60 keV, VMI_low) that show a greater soft-tissue and iodine contrast, and high-energy VMIs (> 90 keV, VMI_high) that reduce beam hardening. VMIs in the mid-range (e. g., between 65 and 70 keV) have been suggested as a working equivalent of polychromatic images at 120 kVp [12, 13].

Other more investigational reconstructions include virtual non-calcium images, electron density images, and Zeff images. While the latter two are thought to be useful for radiation therapy planning, virtual non-calcium images subtract all calcium-associated attenuation from the image (analogously to VUE for iodine) and therefore might prove beneficial for depicting bone marrow edema or cellular infiltration in oncologic diseases.

Clinical applications

The following section will include applications of DECT-derived images for different body regions and indications. At the end of each subsection, a short summary of feasible clinical applications is provided.

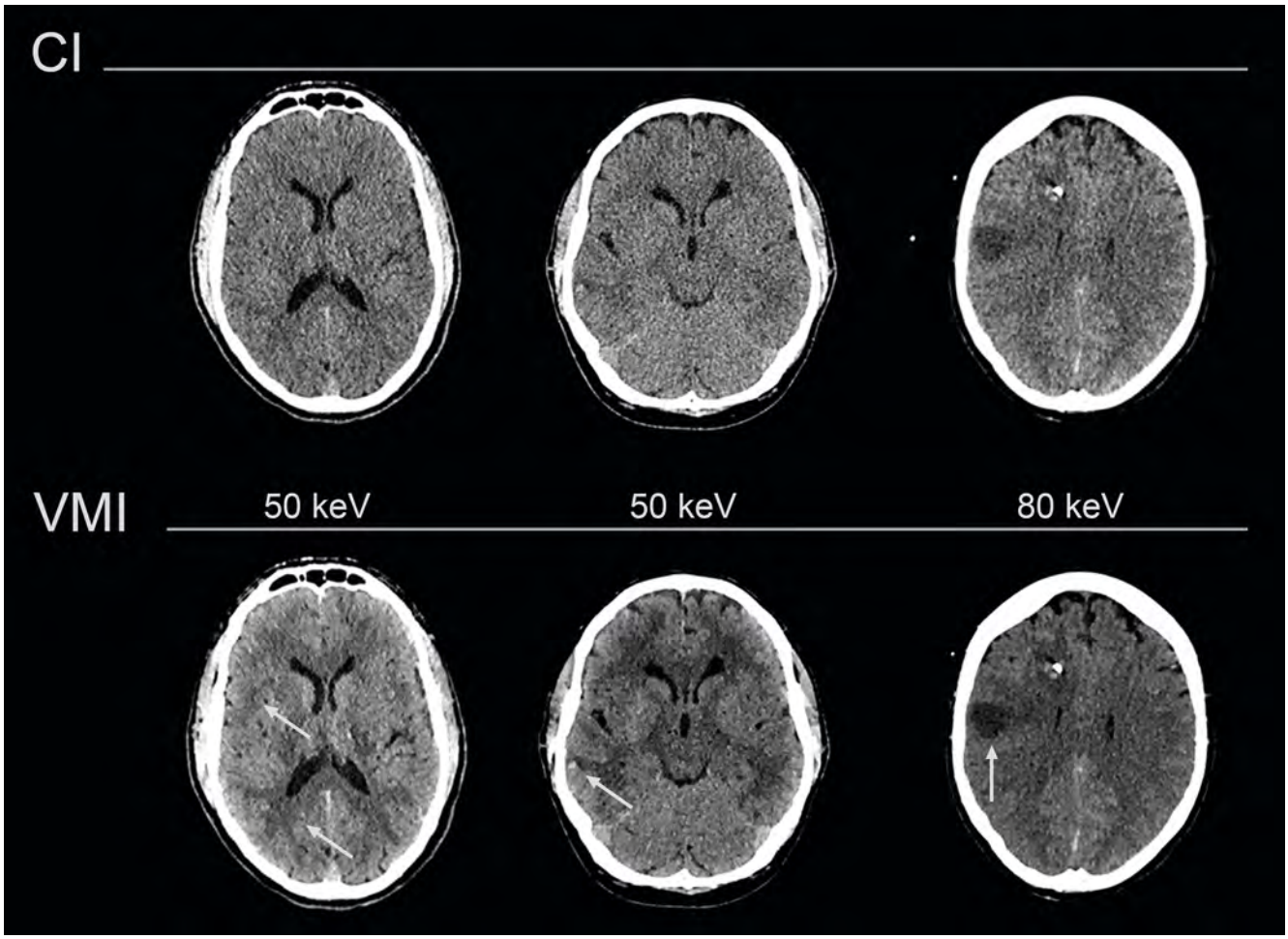

▶ **Fig. 2** Image examples showing improved gray-white matter differentiation (left), increased contrast and conspicuity of intracerebral hemorrhage (center), and better delineation of cerebral infarction (right) in dual-energy CT-derived virtual monoenergetic images (VMI) at different energy levels compared to conventional images (CI).

Neuroradiology

Detection of intracranial hemorrhage and identification of a distortion of grey-white matter differentiation are naturally among the key objectives of an unenhanced CT scan of the head. However, the latter is often found to be challenging as differences between grey and white matter are in the order of 10 HU. This in turn justifies and requires a relatively high radiation dose to minimize image noise. In this instance, low-energy VMIs have been reported to be instrumental, as they allow for an improved contrast between grey and white matter (▶ **Fig. 2**). Most previous publications investigating this topic concluded that virtual keV levels in the range of 50–65 keV would be optimal for enhanced grey-white matter differentiation [14–16]. Using such image reconstructions, a radiation dose reduction of up to 20 % appears justifiable without image quality impairment [16]. In this context, the following thoughts require consideration: A) Some technological DECT implementations, particularly earlier generations, demonstrate a notable increase in image noise with photon energies decreasing towards 40 keV. A balance has to be determined that ensures the increase in contrast is not compromised by an accompanying increase in noise. B) When moving to a lower keV, blooming of calcific structures is a well observed phenomenon. This possibly impairs assessment of the subcalvarial space and hence requires careful consideration. While studies suggested both improvements in quantitative image metrics and image quality in unremarkable cranial CT examinations, some studies also denoted improved detection and delineation of edematous and/or hemorrhagic areas [17–19]. Furthermore, low keV VMIs can improve vascular assessment, e. g., in the case of suspected stroke. This is discussed in detail in the section “cardiovascular imaging”.

Another common challenge in cranial CT examinations is the differentiation between blood and iodine after endovascular treatment of ischemic stroke or aneurysm. For this purpose, VUE images have been reported to be helpful as they eliminate iodine-associated attenuation. Therefore, if hyperattenuating material remains in these images within the brain parenchyma space, it is likely related to blood [20, 21] as opposed to postinterventional contrast material accumulation. A meta-analysis including 204 patients from nine studies on that topic concluded that DECT had a sensitivity and specificity for differentiation between

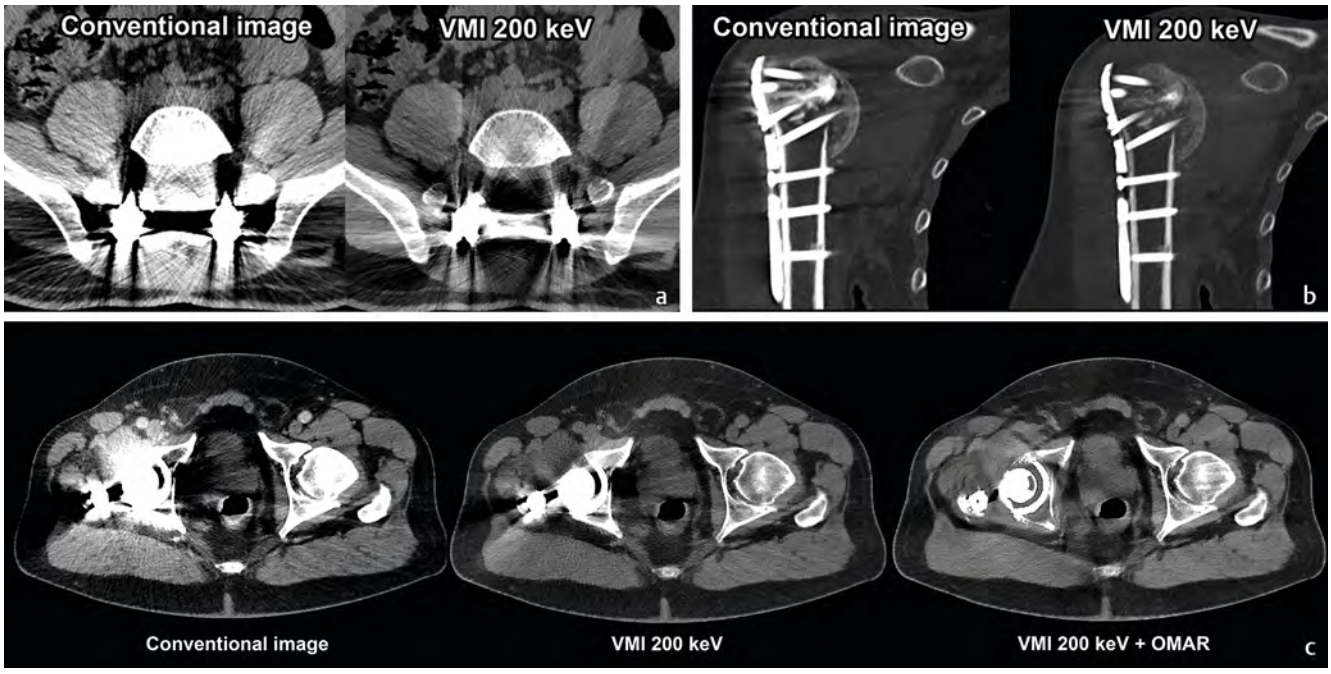

▶ **Fig. 3** **a** Image example depicting artifact reduction in a patient with orthopedic hardware in the lower lumbar spine by means of virtual monoenergetic images (VMI) at 200 keV. Reduction of hypodense streak artifacts with improvement of the paravertebral compartments can be clearly seen. **b** Artifact reduction in a patient with plate osteosynthesis following traumatic fracture of the proximal humerus. Virtual monoenergetic images (VMI) at 200 keV effectively reduce artifacts, allowing for an improved assessment of the remaining fracture lines as well as the osseous tissue surrounding the fixating screws. **c** Different approaches to artifact reduction in a patient with right-sided, total hip replacement. The conventional image depicts pronounced hyperattenuating artifacts surrounding the implant and hypoattenuating artifacts superimposing the organs of the lower pelvis (left side). Virtual monoenergetic images (VMI) at 200 keV show marked reduction of artifacts with improved periprosthetic as well as pelvic assessment (center image). The combination of VMI with an artifact reduction algorithm (OMAR) yields the best possible reduction of artifacts and adequate visualization of the acetabular bone as well as the lower pelvis (right side).

hemorrhage and contrast media or small calcifications of 96 % and 98 %, respectively [22].

Besides the above-mentioned clinical applications of DECT for neuroradiology, a more generic use that will be covered extensively in the "Musculoskeletal Imaging" section is the reduction of artifacts. In the context of neuroradiology, DECT-derived metal artifact reduction has been suggested to improve visualization in patients who underwent clipping or coiling of intracranial aneurysms. High-energy VMIs facilitate the reduction of artifacts. However, in the case of vascular assessment, a balance between the accompanying decline in intravascular contrast and artifact reduction is key. Therefore, in this specific case, the suggested optimal keV levels are not as high as those in musculoskeletal applications and mostly range between 100 and 120 keV [23–25]. Other publications focusing on the assessment of the surrounding brain parenchyma as opposed to vessels suggested higher keV levels accordingly [26].

Key clinical applications: Neuroradiology

1. *Improved grey-white matter differentiation in low-keV VMIs (50–65 keV) with potential for radiation dose reduction*
2. *Improved visualization of hypodense (e. g., ischemia) and hyperdense (e. g., hemorrhage) brain lesions*
3. *Differentiation between intracranial hemorrhage and contrast media*
4. *Reduction of artifacts in patients who underwent intracranial coiling and/or clipping (optimal keV levels need to be adjusted for assessment of the surrounding vessels (lower) or the parenchyma (higher))*

Musculoskeletal imaging

CT is one of the key modalities in acute trauma and fracture imaging. The DECT use case in musculoskeletal imaging with the greatest clinical relevance and impact, for which there is a large body of evidence, is the use of high keV irradiation VMIs to reduce artifacts associated with orthopedic hardware. Moving towards higher energies in VMIs decreases the probability for complete absorption of a photon and the risk for an unsampled or undersampled region surrounding any implant resulting in hypodense streaks. The value of this approach has been investigated in different use cases [27, 28]. Research data suggests a benefit from VMIs with regards to artifacts caused by nearly all types of implants (▶ **Fig. 3a–c**). Most groups suggest implant-specific adjustments of keV levels in order to balance the degree of artifact reduction versus the loss of soft-tissue contrast encountered in high keV imaging [27, 28].

The effectiveness of VMI-enabled artifact reduction appears limited in very dense materials (e. g., in hip protheses or endovascular coils). Here, a particular benefit has been shown for combining high-energy VMIs and dedicated iterative reconstruction algo-

rithms for metal artifact reduction (i. e., MAR; ▶ **Fig. 3c**) [29]. This combination currently represents the strongest means for artifact reduction in DECT imaging (together with optimized imaging protocols).

Another well-established application of DECT in musculoskeletal imaging employs material-specific maps for uric acid in suspected (or clinically proven) gout arthritis [30–32]. These maps are typically evaluated in a fused manner that allows for visualization of uric acid deposits. However, care has to be taken as tendon sheaths and/or cartilage may mimic the attenuation characteristics of uric acid and, therefore, are indicated as uric acid on such reconstructions (▶ **Fig. 4**).

Further suggested applications include an improvement in the imaging of vertebral disc herniation [33] as well as the detection of bone bruise on CT imaging [34–36] (the latter by means of virtual non-calcium images). However, according to the opinion of the authors of this article, these applications are not yet sufficiently validated to allow broad clinical application outside of scientific studies and/or experienced centers.

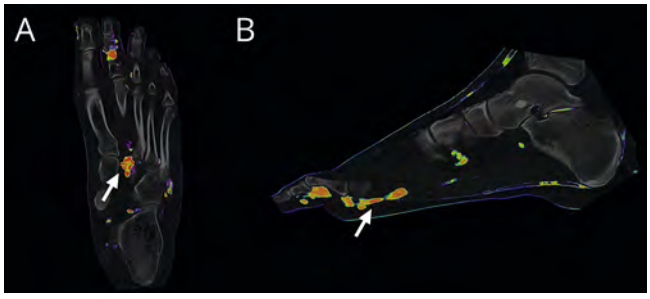

▶ **Fig. 4** **A** Uric acid overlay images showing gout adjacent to the tarsometatarsal joints (arrow) and the proximal interphalangeal joint of the second toe. **B** Calcifications of the plantar aponeurosis, mimicking uric acid deposits.

Key clinical applications: musculoskeletal imaging

1. *Artifact reduction in patients with orthopedic implants using high-keV virtual monoenergetic images exclusively or in combination with dedicated metal artifact-reduction algorithms*
2. *DECT-derived uric acid overlay images for the depiction of urate deposition in patients with gout*

Cardiovascular imaging

Following its capabilities of increasing iodine contrast by means of low keV VMI and subtracting iodine-related attenuation components, DECT has been investigated for various clinical use cases in the field of vascular imaging. For pulmonary embolism, DECT-derived VMI have been shown to yield superior contrast and increase detection, diagnostic certainty, and delineation of thromboembolism [37–39]. Those reconstructions are particularly helpful for salvaging the diagnostic assessability of examinations with suboptimal contrast within the pulmonary arteries [40] (▶ **Fig. 5**). Besides low-keV VMIs yielding superior vessel contrast, iodine maps can be used for the assessment of pulmonary embolism by depicting areas of hypoperfusion within the lung parenchyma. This can be of use both in the acute setting as well as in patients with suspected chronic thromboembolic pulmonary hypertension [41, 42].

One particular use case for DECT in vascular imaging that has been evaluated in the literature is the assessment of aortic endografts. Here, iodine images and VMIs at low energies yielded improved detection of endoleaks depicted as contrast media leakage in the aneurysm sac [43, 44]. Moreover, VUE images showed high sensitivity and specificity for endoleaks in aneurysm graft assessment when used instead of true unenhanced images, enabling differentiation between contrast media and hyperattenuation caused by other causes e. g., calcifications or hemorrhagic deposits. Chandarana et al. suggested that VUE and 80 kVp acquisitions from a dual-source scanner derived from one

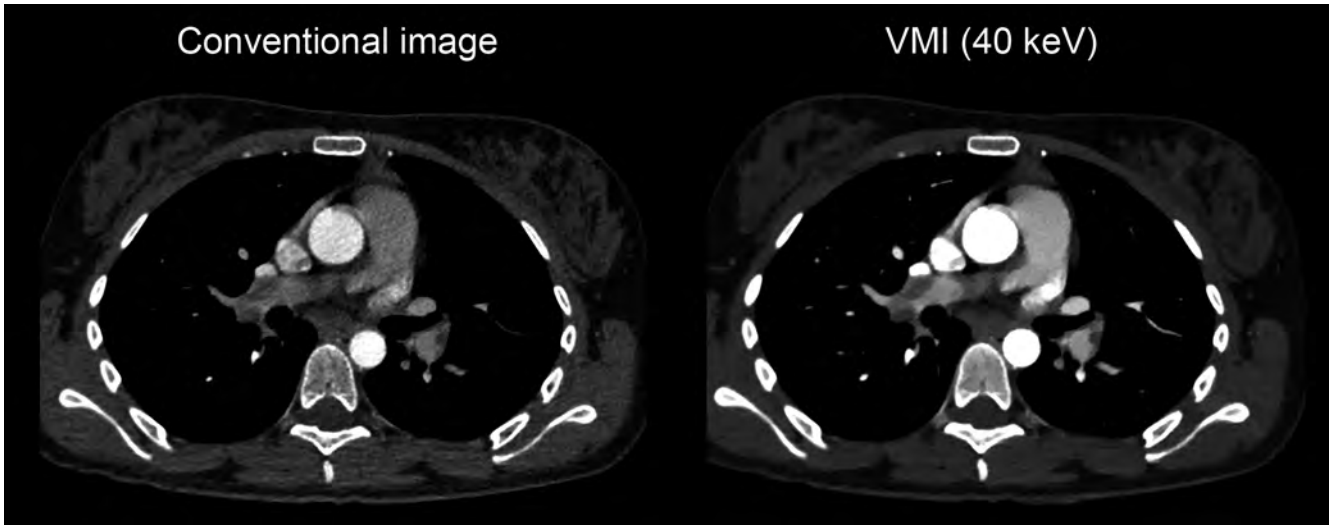

▶ **Fig. 5** Patient with suspected pulmonary embolism. Conventional image shows severely impacted visualization due to suboptimal contrast of the pulmonary arteries. Virtual monoenergetic image (VMI) at 40 keV (right) salvages diagnostic quality by increasing the iodine contrast in the pulmonary arteries, allowing confident delineation of pulmonary emboli.

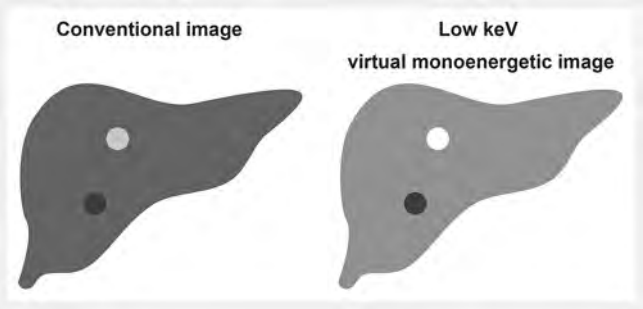

▶ **Fig. 6** Schematic diagram showing increased contrast and conspicuity of hypo- and hyperattenuating liver lesions attained in low keV virtual monoenergetic images. Improved delineation of hypoattenuating lesions is achieved by increased contrast of the surrounding parenchyma, whereas delineation of hyperattenuating lesions is improved by increased attenuation of the lesion itself.

60-second phase might be sufficient for endovascular aneurysm repair assessment [45]. Another important challenge for vascular imaging is the differentiation of contrast material from hemorrhage, e. g., in the assessment of vascular hematoma, for which VUE images may be helpful [46].

The capabilities of DECT to yield VUE and virtual high-contrast (i. e., low-energy virtual monoenergetic) images has been suggested to be combined in a "virtual triphasic" acquisition derived from one portal venous phase image, with significant potential for radiation dose reduction due to the possible elimination of two acquisitions [47].

One potential application of DECT in cardiac imaging that has been investigated in various studies is calcium scoring based on VUE images derived from CCTA, which, if accurate, would allow for omission of an unenhanced acquisition and therefore a significantly lower radiation dose. Whereas most studies described a good correlation between coronary artery calcium scores, they also outlined a systematic underestimation of those metrics in VUE [48–51], which can be attributed to the spectral overlap between calcium and iodine, resulting in an erroneous subtraction of calcium-containing voxels in VUE images. As there is no validated model taking into account this underestimation for routine clinical use, further investigation in this regard seems necessary before routine clinical application can be implemented.

Key clinical applications: cardiovascular imaging

1. *Improved assessment of pulmonary embolism in low-keV VMIs*
2. *Restoring diagnostic image quality in angiographic phase examinations with suboptimal contrast using low-keV VMIs*
3. *Assessment of contrast media leakage (e. g., in endograft assessment) and vascular wall hematoma in low keV/iodine images and VUE images, respectively*

Oncologic and organ-specific imaging

Liver

Accurate assessment of the liver parenchyma is paramount to determine the presence or absence of liver metastases and safeguard optimal therapeutic concepts for cancer patients. Due to the limited soft-tissue contrast on CT, the detection of small lesions with subtle enhancement differences compared to the surrounding parenchyma can be hampered. DECT-derived VMIs at low energy levels facilitate improved conspicuity of liver lesions. For hyperattenuating liver lesions, this is achieved by increasing the attenuation of the lesion itself, thereby improving the contrast-to-noise ratio and its conspicuity and detectability [52–55], as schematically depicted in ▶ **Fig. 6**. For hypoattenuating lesions, a better depiction is attained by increasing the attenuation of the surrounding liver parenchyma [56, 57]. In summary, low-keV virtual monoenergetic images sent to the PACS as standard reconstructions in oncologic patients are an easy-to-use screening tool for small, subtle, hypo- and hyperattenuating liver lesions.

Small, intermediate lesions of the liver, which are often called "too small to characterize", present another diagnostic challenge in regard to CT liver imaging. DECT-derived iodine images may help to increase diagnostic confidence when diagnosing such lesions, for example by ruling out any iodine uptake in iodine images. One study found that the classification of such small, intermediate hypoattenuating liver lesions could be improved significantly with the use of iodine images and an iodine-based threshold as compared to conventional images [58]. However, large-scale validation of this quantitative application seems necessary before broad clinical application can be implemented. The same applies to studies that suggested DECT-enabled differentiation of liver lesions, e. g., between small HCCs and metastases based on iodine quantification, which has been investigated only in small cohorts [59, 60].

Kidneys

Renal masses with non-cystic attenuation of equal or greater than 20 HU on contrast-enhanced abdominal CT are a common incidental finding [61]. One study suggested that in > 50 % of adults aged 50 or older, imaging would yield at least one incidental renal mass [62]. The differential diagnoses for such masses include hemorrhagic or proteinaceous cysts as well as solid-enhancing masses. Differentiation between these lesions in monophasic, portal venous phase single-energy CT is hampered by the lack of information on the baseline unenhanced attenuation enabling assessment of lesion enhancement. Consequently, many patients diagnosed with such incidental lesions are recommended to undergo additional multiphasic renal protocol CT or MRI examination. By means of material decomposition, DECT allows differentiation between the attenuation component derived from iodinated contrast material and other non-iodine-related tissue or material components such as protein or blood. This has resulted in a large number of studies that aimed to assess the utility of DECT in characterizing renal lesions, which investigated both the use of virtual unenhanced and iodine images. A meta-analysis of five studies with a total patient number of 367 revealed a sensitivity and specificity of 96.6 and 95.1 %, respectively, for iodine images with respect to determining lesion enhancement [63]. In another study, Meyer et al. showed that virtual unenhanced images allow for accurate renal lesion characterization, albeit with a lower specificity compared to true unenhanced images [64]. Accordingly,

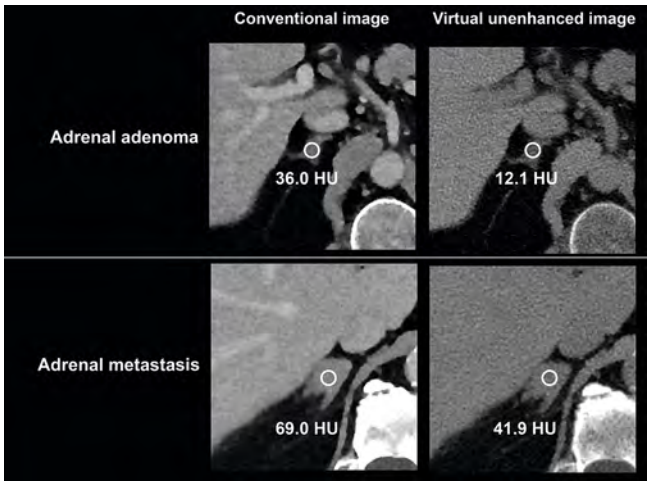

▶ **Fig. 7** Virtual unenhanced images derived from dual-energy CT for differentiation between adrenal adenoma (upper row) and adrenal metastasis (lower row).

Cao et al. recently found that virtual enhancement calculated from the portal venous phase and virtual unenhanced images correctly identified all enhancing lesions within their study cohort, yet noted that in some cases, virtual unenhanced images diverged from true unenhanced image attenuation with regard to the evaluation of cystic lesions [65]. In the clinical routine, virtual unenhanced and iodine images can be used synergistically to rule out enhancement in ambiguous renal lesions. In this instance, previously investigated, scanner-dependent lower limits of detection and quantification of iodine should be consulted when aiming to assess the presence of iodine enhancement [66]. We suggest that the current body of evidence supports using DECT for determining or ruling out enhancement of hyperattenuating renal lesions. More advanced quantitative applications such as differentiation of different subtypes of RCCs have been investigated [67, 68]. However, the corresponding thresholds have not been validated and are prone to a certain variability of iodine quantification [69, 70].

Another, and one of the earliest use cases of DECT in renal imaging is the characterization of renal calculi. Significant evidence is available that indicates that identification of uric acid concrements is possible by means of material-specific maps for uric acid [71–74]. Furthermore, several groups investigated whether stone composition analysis is possible beyond this. However, the body of literature is too small and furthermore too scanner- and protocol-specific to be able to consider this a generally valid method in this context [75, 76].

Adrenal glands

Adrenal nodules are one of the most common incidental findings in abdominal CT with a reported prevalence of up to 7 % [77]. In the overall population, the majority of these adrenal nodules are known to represent benign adrenal adenomas. However, in cancer patients, there is an increased risk that these lesions represent metastatic spread to the adrenal glands. Lipid-rich adenomas are characterized by the presence of macroscopic fat. This can be determined by an unenhanced CT attenuation threshold of 10 HU, which has been suggested to yield a sensitivity/specificity of 71 %/98 % [78], or by a signal loss on chemical shift MRI. It has been described that overall, around 70 % of adenomas can be determined as lipid-rich following an unenhanced attenuation of < 10 HU [79–82]. However, in most instances, adrenal incidentalomas are detected in CT examinations not tailored for such an assessment due to a lack of unenhanced or delayed phase image acquisitions, based on radiation protection considerations. Consequently, definitive characterization and exclusion of metastatic spread would require additional imaging such as dedicated CT for adrenal assessment comprising an unenhanced and delayed phase, or MRI with in-and-out-of-phase imaging. DECT-derived VUE and iodine images have been extensively investigated scientifically for one-stop-shop characterization of incidental adrenal nodules in portal venous phase abdominal CT examinations [83–89]. As discussed before, VUE images allow for estimation of the true unenhanced image attenuation. Therefore, a VUE attenuation of < 10 HU calculated from portal venous phase images is highly indicative of lipid-rich adrenal adenoma. One problem that has been addressed in the literature is that virtual unenhanced image attenuation shows a tendency towards overestimation of true unenhanced image attenuation in adrenal adenomas [89–92], limiting the sensitivity in determining their lipid-rich nature. Different ways of mitigating this issue have been suggested, most notably increasing the 10 HU threshold. Another means of addressing this issue has been suggested, i. e., including iodine measurements in a multiparametric approach, which yielded promising results. However, these monocentric, retrospective results have not been validated yet [89]. As virtual unenhanced attenuation is known to show intra-patient variation between different DECT platforms, state-of-the-art, device-specific data should be consulted when using quantitative DECT measurements as stated above for the characterization of incidental adrenal nodules [93]. ▶ **Fig. 7** illustrates an example of adrenal differentiation using VUE images.

Metastasis detection

With its large overall volume and high physical density, the skeletal muscle is notoriously hard to assess on conventional CT, qualifying it as one of the “blind spots” of oncologic staging and follow-up CT. Due to several underlying factors, the human skeletal muscle is relatively resistant to hematogenous metastatic spread of oncologic diseases. However, for some malignant diseases such as malignant melanoma, a higher probability of skeletal muscle metastasis has been described [94]. In oncologic imaging, the detection of such distant metastases is important since the new appearance of metastatic lesions may indicate the necessity for the adjustment of treatment concepts. Several studies have described an improved sensitivity for skeletal muscle metastases in DECT-derived reconstructions highlighting iodine contrast, such as low keV virtual monoenergetic images and iodine overlay images, in which the iodine content is color-coded and merged with underlying grey-scale conventional images [95, 96].

The underlying rationale is that images highlighting the iodine-related attenuation allow for the differentiation of iodine-related attenuation components of enhancing metastatic lesions vs.

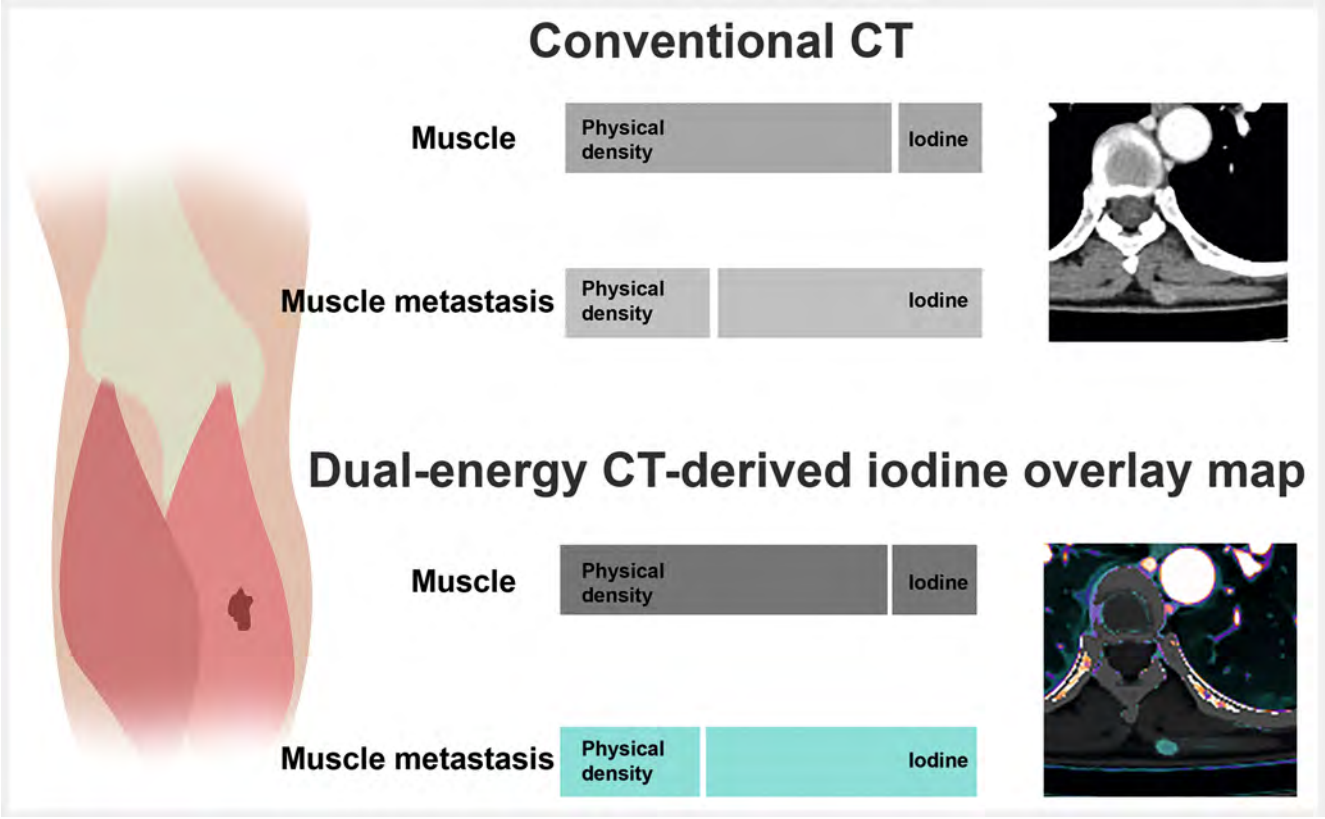

▶ **Fig. 8** Simplified schematic illustration of attenuation components of skeletal muscle metastases and surrounding muscle parenchyma including an exemplary case of skeletal muscle metastasis on conventional and iodine overlay images in a patient with melanoma.

physical density-related attenuation components of circumjacent muscle, which may be almost indistinguishable on conventional images (▶ **Fig. 8**). Therefore, these images may qualify as screening tools for patients with oncologic diseases or disease stages, respectively, that yield a higher pre-test probability for metastatic spread to the muscle. Finally, in a prospective evaluation of patients with occult cancer, it was described that spectral reconstructions may improve the confidence of radiologists in characterizing lesions, thereby making it possible to minimize correlative imaging [97].

Other applications

The substantially increased attenuation of iodinated contrast material in low keV virtual monoenergetic reconstructions can not only be used to increase conspicuity and detectability of organ-specific lesions as described above, but also to lower the overall amount of contrast media that has to be applied for attaining sufficient visualization (▶ **Fig. 9**). In a study by Nagayama et al., it was shown that VMIs from 40 to 55 keV allowed for a reduction of contrast media dose by 50 % in multiphase liver CT [98]. In another study, VMIs at 40 keV were reported to yield organ and vessel assessment comparable to a full-dose protocol in portal venous phase abdominal CT at a 50 % lower iodine concentration load [99]. In regard to aortic angiography with 50 % contrast material reduction, DECT-derived VMIs ranging from 40 to 60 keV were reported to yield similar image quality as normal iodine contrast material doses [100]. Lastly, Agrawal et al. reported a significantly higher attenuation and CNR in low-energy VMI CTA with a reduction of contrast media to 24 g/l compared to standard-dose CTA (33 g/l) [101]. Based on the above-mentioned evidence, a minimum volume of 50 ml contrast media (depending on the specific contrast media administration protocol (i. e., bolus length)) in combination with low keV VMI appears to be a valid strategy in patients at an increased risk for contrast media-associated nephropathy or other dose-dependent adverse events.

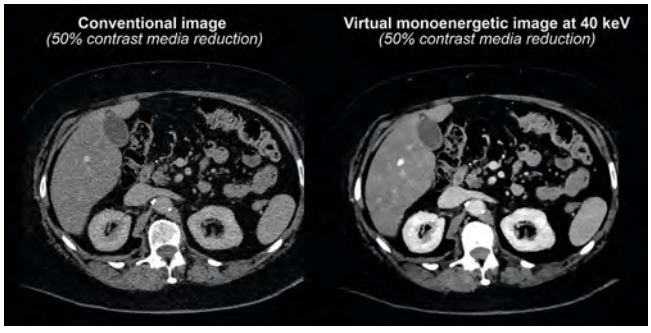

▶ **Fig. 9** Cross-sectional image of a portal venous phase CT scan of the upper abdomen with a contrast media reduction of 50 %. The left image represents the conventional image, whereas the right image with only poor contrast enhancement depicts the corresponding virtual monoenergetic image at 40 keV, restoring adequate tissue contrast.

Key clinical applications: Oncologic and organ-specific imaging

1. *Liver:*
   a) *Low-keV VMI as a screening tool for hypo- and hyperattenuating liver lesions in cancer patients;*
   b) *Iodine maps for increased confidence in determining the cystic nature in small hypodense liver lesions.*
2. *Kidneys:*
   a) *Characterization of ambiguous renal lesions as cystic vs. contrast-enhancing using iodine maps and virtual unenhanced images.*
   b) *Detection and characterization of kidney stones*
3. *Adrenals: Identification of incidental adenoma with virtual unenhanced images (consult literature for scanner-specific, adjusted thresholds)*
4. *Detection of skeletal muscle metastases in iodine overlay images in patients with increased pretest probability*
5. *Contrast media reduction with low-keV virtual monoenergetic images to antagonize iodine contrast deterioration*

Conclusion

Dual-energy CT has undergone broad scientific evaluation of various potential use cases. The most frequently used reconstructions are virtual monoenergetic images to improve contrast, iodine maps to quantify perfusion at time point of imaging, and virtual unenhanced images to approximate true non-contrast acquisitions. Some of those use cases warrant clinical application with important benefits for the radiological routine, whereas others showed promise in initial investigations, yet require further validation.

Conflict of Interest

Nils Große Hokamp received speaker's honoraria from Philips Healthcare. Nils Große Hokamp receives research support from Philips Healthcare. Nils Große Hokamp is consultant to Bristol Myers Squibb. Nils Große Hokamp received speaker honoraria from Amboss. David Zopfs received speaker's honoraria from Philips Healthcare and Amboss. Simon Lennartz received speaker's and author's honoraria from Amboss.

References

[1] Alvarez RE, Macovski A. Energy-selective reconstructions in X-ray computerised tomography. Phys Med Biol 1976; 21: 002. doi:10.1088/0031-9155/21/5/002

[2] Hounsfield GN. Computerized transverse axial scanning (tomography): I. Description of system. Br J Radiol 1973; 46: 1016–1022. doi:10.1259/0007-1285-46-552-1016

[3] Flohr TG, McCollough CH, Bruder H. First performance evaluation of a dual-source CT (DSCT) system. Eur Radiol 2006; 16: 256

[4] Petersilka M, Bruder H, Krauss B et al. Technical principles of dual source CT. Eur J Radiol 2008; 68: 362

[5] Schlemmer H-P. The Eye of the CT Scanner: The story of learning to see the invisible or from the fluorescent screen to the photon-counting detector. Fortschr Röntgenstr 2021; 193: 1034–1049. doi:10.1055/a-1308-2693

[6] Siegel MJ, Kaza RK, Bolus DN et al. White Paper of the Society of Computed Body Tomography and Magnetic Resonance on Dual-Energy CT, Part 1.
J Comput Assist Tomogr 2016; 40: 841–845. doi:10.1097/RCT.0000000000000531

[7] Mccollough CH, Leng S, Yu L et al. Dual- and Multi-Energy CT: Principles, Technical Approaches, and Clinical Applications. Radiology 2015; 276: 637–653. doi:10.1148/radiol.2015142631

[8] Willemink MJ, Persson M, Pourmorteza A et al. Photon-counting CT: Technical principles and clinical prospects. Radiology 2018; 289: 293–312. doi:10.1148/radiol.2018172656

[9] Parakh A, Lennartz S, An C et al. Dual-Energy CT Images: Pearls and Pitfalls. RadioGraphics 2021; 41: 98–119. doi:10.1148/rg.2021200102

[10] Jacobsen MC, Cressman ENK, Tamm EP et al. Dual-energy CT: Lower limits of iodine detection and quantification. Radiology 2019; 292: 414–419. doi:10.1148/radiol.2019182870

[11] Toepker M, Moritz T, Krauss B et al. Virtual non-contrast in second-generation, dual-energy computed tomography: reliability of attenuation values. Eur J Radiol 2012; 81: e398–e405. doi:10.1016/j.ejrad.2011.12.011

[12] Reimer RP, Große Hokamp N, Fehrmann Efferoth A et al. Virtual monoenergetic images from spectral detector computed tomography facilitate washout assessment in arterially hyper-enhancing liver lesions. Eur Radiol 2021; 31: 3468–3477. doi:10.1007/s00330-020-07379-3

[13] Matsumoto K, Jinzaki M, Tanami Y et al. Virtual monochromatic spectral imaging with fast kilovoltage switching: improved image quality as compared with that obtained with conventional 120-kVp CT. Radiology 2011; 259: 257

[14] Pomerantz SR, Kamalian S, Zhang D et al. Virtual Monochromatic Reconstruction of Dual-Energy Unenhanced Head CT at 65–75 keV Maximizes Image Quality Compared with Conventional Polychromatic CT. Radiology 2013; 266: 318–325. doi:10.1148/radiol.12111604

[15] Neuhaus V, Abdullayev N, Große Hokamp N et al. Improvement of Image Quality in Unenhanced Dual-Layer CT of the Head Using Virtual Monoenergetic Images Compared With Polyenergetic Single-Energy CT. Invest Radiol 2017; 52: 470–476. doi:10.1097/RLI.0000000000000367

[16] Reimer RP, Flatten D, Lichtenstein T et al. Virtual Monoenergetic Images from Spectral Detector CT Enable Radiation Dose Reduction in Unenhanced Cranial CT. Am J Neuroradiol 2019. doi:10.3174/ajnr.A6220

[17] Lennartz S, Laukamp KR, Neuhaus V et al. Dual-layer detector CT of the head: Initial experience in visualization of intracranial hemorrhage and hypodense brain lesions using virtual monoenergetic images. Eur J Radiol 2018; 108: 177–183. doi:10.1016/j.ejrad.2018.09.010

[18] Cho SB, Baek HJ, Ryu KH et al. Initial clinical experience with dual-layer detector spectral CT in patients with acute intracerebral haemorrhage: A single-centre pilot study. PLoS One 2017; 12: e0186024. doi:10.1371/journal.pone.0186024

[19] van Ommen F, Dankbaar JW, Zhu G et al. Virtual monochromatic dual-energy CT reconstructions improve detection of cerebral infarct in patients with suspicion of stroke. Neuroradiology 2021; 63: 41–49. doi:10.1007/s00234-020-02492-y

[20] Tijssen MPM, Hofman PAM, Stadler AAR et al. The role of dual energy CT in differentiating between brain haemorrhage and contrast medium after mechanical revascularisation in acute ischaemic stroke. Eur Radiol 2014; 24: 834–840. doi:10.1007/s00330-013-3073-x

[21] Gupta R, Phan CM, Leidecker C et al. Evaluation of Dual-Energy CT for Differentiating Intracerebral Hemorrhage from Iodinated Contrast Material Staining. Radiology 2010; 257: 205–211. doi:10.1148/radiol.10091806

[22] Choi Y, Shin N-Y, Jang J et al. Dual-energy CT for differentiating acute intracranial hemorrhage from contrast staining or calcification: a meta-analysis. Neuroradiology 2020; 62: 1617–1626. doi:10.1007/s00234-020-02486-w

[23] Nair JR, Burrows C, Jerome S et al. Dual energy CT: a step ahead in brain and spine imaging. Br J Radiol 2020; 93: 20190872. doi:10.1259/bjr.20190872

[24] Winklhofer S, Hinzpeter R, Stocker D et al. Combining monoenergetic extrapolations from dual-energy CT with iterative reconstructions: reduction of coil and clip artifacts from intracranial aneurysm therapy. Neuroradiology 2018; 60: 281–291. doi:10.1007/s00234-018-1981-9

[25] Dunet V, Bernasconi M, Hajdu SD et al. Impact of metal artifact reduction software on image quality of gemstone spectral imaging dual-energy cerebral CT angiography after intracranial aneurysm clipping. Neuroradiology 2017; 59: 845–852. doi:10.1007/s00234-017-1871-6

[26] Zopfs D, Lennartz S, Pennig L et al. Virtual monoenergetic images and post-processing algorithms effectively reduce CT artifacts from intracranial aneurysm treatment. Sci Rep 2020; 10: 6629. doi:10.1038/s41598-020-63574-8

[27] Mallinson PI, Coupal TM, McLaughlin PD et al. Dual-Energy CT for the Musculoskeletal System. Radiology 2016; 281: 690–707. doi:10.1148/radiol.2016151109

[28] Albrecht MH, Vogl TJ, Martin SS et al. Review of Clinical Applications for Virtual Monoenergetic Dual-Energy CT. Radiology 2019; 293: 260–271. doi:10.1148/radiol.2019182297

[29] Große Hokamp N, Hellerbach A, Gierich A et al. Reduction of Artifacts Caused by Deep Brain Stimulating Electrodes in Cranial Computed Tomography Imaging by Means of Virtual Monoenergetic Images, Metal Artifact Reduction Algorithms, and Their Combination. Invest Radiol 2018; 53: 424–431. doi:10.1097/RLI.0000000000000460

[30] Chou H, Chin TY, Peh WCG. Dual-energy CT in gout – A review of current concepts and applications. J Med Radiat Sci 2017; 64: 41–51. doi:10.1002/jmrs.223

[31] Bongartz T, Glazebrook KN, Kavros SJ et al. Dual-energy CT for the diagnosis of gout: an accuracy and diagnostic yield study. Ann Rheum Dis 2015; 74: 1072–1077. doi:10.1136/annrheumdis-2013-205095

[32] Desai MA, Peterson JJ, Garner HW et al. Clinical Utility of Dual-Energy CT for Evaluation of Tophaceous Gout. RadioGraphics 2011; 31: 1365–1375. doi:10.1148/rg.315115510

[33] Booz C, Nöske J, Martin SS et al. Virtual Noncalcium Dual-Energy CT: Detection of Lumbar Disk Herniation in Comparison with Standard Grayscale CT. Radiology 2019; 290: 446–455. doi:10.1148/radiol.2018181286

[34] Gosangi B, Mandell JC, Weaver MJ et al. Bone Marrow Edema at Dual-Energy CT: A Game Changer in the Emergency Department. RadioGraphics 2020; 40: 859–874. doi:10.1148/rg.2020190173

[35] Diekhoff T, Hermann KG, Pumberger M et al. Dual-energy CT virtual non-calcium technique for detection of bone marrow edema in patients with vertebral fractures: A prospective feasibility study on a single-source volume CT scanner. Eur J Radiol 2017; 87: 59–65. doi:10.1016/j.ejrad.2016.12.008

[36] Ai S, Qu M, Glazebrook KN et al. Use of dual-energy CT and virtual non-calcium techniques to evaluate post-traumatic bone bruises in knees in the subacute setting. Skeletal Radiol 2014; 43: 1289–1295. doi:10.1007/s00256-014-1913-7

[37] Abdellatif W, Ebada MA, Alkanj S et al. Diagnostic Accuracy of Dual-Energy CT in Detection of Acute Pulmonary Embolism: A Systematic Review and Meta-Analysis. Can Assoc Radiol J 2021; 72: 285–292. doi:10.1177/0846537120902062

[38] Kröger JR, Hickethier T, Pahn G et al. Influence of spectral detector CT based monoenergetic images on the computer-aided detection of pulmonary artery embolism. Eur J Radiol 2017; 95: 242–248. doi:10.1016/j.ejrad.2017.08.034

[39] Dane B, Patel H, O'Donnell T et al. Image Quality on Dual-energy CTPA Virtual Monoenergetic Images. Acad Radiol 2018; 25: 1075–1086. doi:10.1016/j.acra.2017.12.012

[40] Leithner D, Wichmann JL, Vogl TJ et al. Virtual Monoenergetic Imaging and Iodine Perfusion Maps Improve Diagnostic Accuracy of Dual-Energy Computed Tomography Pulmonary Angiography With Suboptimal Contrast Attenuation. Invest Radiol 2017; 52: 659–665. doi:10.1097/RLI.0000000000000387

[41] Kroeger JR, Zöllner J, Gerhardt F et al. Detection of patients with chronic thromboembolic pulmonary hypertension by volumetric iodine quantification in the lung-a case control study. Quant Imaging Med Surg 2022; 12: 1121–1129. doi:10.21037/qims-21-229

[42] Hoey ETD, Mirsadraee S, Pepke-Zaba J et al. Dual-Energy CT Angiography for Assessment of Regional Pulmonary Perfusion in Patients With Chronic Thromboembolic Pulmonary Hypertension: Initial Experience. Am J Roentgenol 2011; 196: 524–532. doi:10.2214/Am J Roentgenol.10.4842

[43] Ascenti G, Mazziotti S, Lamberto S et al. Dual-energy CT for detection of endoleaks after endovascular abdominal aneurysm repair: Usefulness of colored iodine overlay. Am J Roentgenol 2011; 196: 1408–1414. doi:10.2214/Am J Roentgenol.10.4505

[44] Javor D, Wressnegger A, Unterhumer S et al. Endoleak detection using single-acquisition split-bolus dual-energy computer tomography (DECT). Eur Radiol 2017; 27: 1622–1630. doi:10.1007/s00330-016-4480-6

[45] Chandarana H, Godoy MC, Vlahos I. Abdominal aorta: evaluation with dual-source dual-energy multidetector CT after endovascular repair of aneurysms—initial observations. Radiology 2008; 249: 692

[46] Si-Mohamed S, Dupuis N, Tatard-Leitman V et al. Virtual versus true non-contrast dual-energy CT imaging for the diagnosis of aortic intramural hematoma. Eur Radiol 2019; 29: 6762–6771. doi:10.1007/s00330-019-06322-5

[47] Lennartz S, Laukamp KR, Tandon Y et al. Abdominal vessel depiction on virtual triphasic spectral detector CT: initial clinical experience. Abdom Radiol 2021; 46: 3501–3511. doi:10.1007/s00261-021-03001-2

[48] Lee HA, Lee YH, Yoon KH et al. Comparison of virtual unenhanced images derived from dual-energy CT with true unenhanced images in evaluation of gallstone disease. Am J Roentgenol 2016; 206: 74–80. doi:10.2214/Am J Roentgenol.15.14570

[49] Song I, Yi JG, Park JH et al. Virtual Non-Contrast CT Using Dual-Energy Spectral CT: Feasibility of Coronary Artery Calcium Scoring. Korean J Radiol 2016; 17: 321. doi:10.3348/kjr.2016.17.3.321

[50] Gassert FG, Schacky CE, Müller-Leisse C et al. Calcium scoring using virtual non-contrast images from a dual-layer spectral detector CT: comparison to true non-contrast data and evaluation of proportionality factor in a large patient collective. Eur Radiol 2021; 31: 6193–6199. doi:10.1007/s00330-020-07677-w

[51] Yamada Y, Jinzaki M, Okamura T et al. Feasibility of coronary artery calcium scoring on virtual unenhanced images derived from single-source fast kVp-switching dual-energy coronary CT angiography. J Cardiovasc Comput Tomogr 2014; 8: 391–400. doi:10.1016/j.jcct.2014.08.005

[52] Große Hokamp N, Höink AJ, Doerner J et al. Assessment of arterially hyper-enhancing liver lesions using virtual monoenergetic images from spectral detector CT: phantom and patient experience. Abdom Radiol 2018; 43: 2066–2074. doi:10.1007/s00261-017-1411-1

[53] Mileto A, Nelson RC, Samei E et al. Dual-energy MDCT in hypervascular liver tumors: effect of body size on selection of the optimal monochromatic energy level. Am J Roentgenol 2014; 203: 1257–1264. doi:10.2214/Am J Roentgenol.13.12229

[54] Shuman WP, Green DE, Busey JM et al. Dual-energy liver CT: Effect of monochromatic imaging on lesion detection, conspicuity, and contrast-to-noise ratio of hypervascular lesions on late arterial phase. Am J Roentgenol 2014; 203: 601–606. doi:10.2214/Am J Roentgenol.13.11337

[55] Altenbernd J, Heusner TA, Ringelstein A et al. Dual-energy-CT of hypervascular liver lesions in patients with HCC: Investigation of image quality

and sensitivity. Eur Radiol 2011; 21: 738–743. doi:10.1007/s00330-010-1964-7

[56] Husarik DB, Gordic S, Desbiolles L et al. Advanced Virtual Monoenergetic Computed Tomography of Hyperattenuating and Hypoattenuating Liver Lesions: Ex-Vivo and Patient Experience in Various Body Sizes. Invest Radiol 2015; 50: 695–702. doi:10.1097/RLI.0000000000000171

[57] Husarik DB, Gordic S, Desbiolles L et al. Advanced Virtual Monoenergetic Computed Tomography of Hyperattenuating and Hypoattenuating Liver Lesions. Invest Radiol 2015; 50: 695–702. doi:10.1097/RLI.0000000000000171

[58] Patel BN, Rosenberg M, Vernuccio F et al. Characterization of Small Incidental Indeterminate Hypoattenuating Hepatic Lesions: Added Value of Single-Phase Contrast-Enhanced Dual-Energy CT Material Attenuation Analysis. Am J Roentgenol 2018; 211: 571–579. doi:10.2214/Am J Roentgenol.17.19170

[59] Kaltenbach B, Wichmann JL, Pfeifer S et al. Iodine quantification to distinguish hepatic neuroendocrine tumor metastasis from hepatocellular carcinoma at dual-source dual-energy liver CT. Eur J Radiol 2018; 105: 20–24. doi:10.1016/j.ejrad.2018.05.019

[60] Laroia ST, Yadav K, Kumar S et al. Material decomposition using iodine quantification on spectral CT for characterising nodules in the cirrhotic liver: a retrospective study. Eur Radiol Exp 2021; 5: 22. doi:10.1186/s41747-021-00220-6

[61] Berland LL, Silverman SG, Gore RM. Managing incidental findings on abdominal CT: white paper of the ACR incidental findings committee. J Am Coll Radiol 2010; 7: 754

[62] Silverman SG, Israel GM, Herts BR et al. Management of the incidental renal mass. Radiology 2008; 249: 16

[63] Salameh J, Mcinnes MDF, Mcgrath TA et al. Diagnostic Accuracy of Dual-Masses: Systematic Review and Meta-Analysis. AJR Am J Roentgenol 2019; 212: W100–W105. doi:10.2214/AJR.18.20527

[64] Meyer M, Nelson RC, Vernuccio F et al. Virtual Unenhanced Images at Dual-Energy CT: Influence on Renal Lesion Characterization. Radiology 2019; 291: 381–390. doi:10.1148/radiol.2019181100

[65] Cao J, Lennartz S, Pisuchpen N et al. Renal Lesion Characterization by Dual-Layer Dual-Energy CT: Comparison of Virtual and True Unenhanced Images. Am J Roentgenol 2022; 219: 614–623. doi:10.2214/Am J Roentgenol.21.27272

[66] Jacobsen MC, Cressman ENK, Tamm EP et al. Dual-Energy CT: Lower Limits of Iodine Detection and Quantification. Radiology 2019; 292: 414–419. doi:10.1148/radiol.2019182870

[67] Mileto A, Marin D, Alfaro-Cordoba M et al. Iodine quantification to distinguish clear cell from papillary renal cell carcinoma at dual-energy multidetector CT: A multireader diagnostic performance study. Radiology 2014; 273: 813–820. doi:10.1148/radiol.14140171

[68] Graser A, Becker CR, Staehler M et al. Single-phase dual-energy CT allows for characterization of renal masses as benign or malignant. Invest Radiol 2010; 45: 399–405. doi:10.1097/RLI.0b013e3181e33189

[69] Lennartz S, Abdullayev N, Zopfs D et al. Intra-individual consistency of spectral detector CT-enabled iodine quantification of the vascular and renal blood pool. Eur Radiol 2019; 29. doi:10.1007/s00330-019-06266-w

[70] Zopfs D, Reimer RP, Sonnabend K et al. Intraindividual consistency of iodine concentration in dual-energy computed tomography of the chest and abdomen. Invest Radiol 2021; 56: 181–187. doi:10.1097/RLI.0000000000000724

[71] Nestler T, Haneder S, Hokamp NG. Modern imaging techniques in urinary stone disease. Curr Opin Urol 2019; 29: 81–88. doi:10.1097/MOU.0000000000000572

[72] Große Hokamp N, Lennartz S, Salem J et al. Dose independent characterization of renal stones by means of dual energy computed tomography and machine learning: an ex-vivo study. Eur Radiol 2020; 30: 1397–1404. doi:10.1007/s00330-019-06455-7

[73] Spek A, Strittmatter F, Graser A et al. Dual energy can accurately differentiate uric acid-containing urinary calculi from calcium stones. World J Urol 2016; 34: 1297–1302. doi:10.1007/s00345-015-1756-4

[74] Jendeberg J, Thunberg P, Popiolek M et al. Single-energy CT predicts uric acid stones with accuracy comparable to dual-energy CT-prospective validation of a quantitative method. Eur Radiol 2021; 31: 5980–5989. doi:10.1007/s00330-021-07713-3

[75] Hokamp NG, Salem J, Hesse A et al. Low-Dose Characterization of Kidney Stones Using Spectral Detector Computed Tomography: An Ex Vivo Study. Invest Radiol 2018; 53: 457–462. doi:10.1097/RLI.0000000000000468

[76] Hidas G, Eliahou R, Duvdevani M et al. Determination of Renal Stone Composition with Dual-Energy CT: In Vivo Analysis and Comparison with X-ray Diffraction. Radiology 2010; 257: 394–401. doi:10.1148/radiol.10100249

[77] Bovio S, Cataldi A, Reimondo G et al. Prevalence of adrenal incidentaloma in a contemporary computerized tomography series. J Endocrinol Investig 2006; 29: 298–302

[78] Boland GW, Lee MJ, Gazelle GS et al. Characterization of adrenal masses using unenhanced CT: an analysis of the CT literature. Am J Roentgenol 1998; 171: 201

[79] Boland GW, Lee MJ, Gazelle GS et al. Characterization of adrenal masses using unenhanced CT: an analysis of the CT literature. Am J Roentgenol 1998; 171: 201–204. doi:10.2214/ajr.171.1.9648789

[80] Mayo-Smith WW, Song JH, Boland GL et al. Management of Incidental Adrenal Masses: A White Paper of the ACR Incidental Findings Committee. J Am Coll Radiol 2017; 14: 1038–1044. doi:10.1016/j.jacr.2017.05.001

[81] Caoili EM, Korobkin M, Francis IR. Adrenal masses: characterization with combined unenhanced and delayed enhanced CT. Radiology 2002; 222: 629

[82] Schieda N, Siegelman ES. Update on CT and MRI of Adrenal Nodules. Am J Roentgenol 2017; 208: 1206–1217. doi:10.2214/Am J Roentgenol.16.17758

[83] Kim YK, Park BK, Kim CK et al. Adenoma characterization: Adrenal protocol with dual-energy CT. Radiology 2013; 267: 155–163. doi:10.1148/radiol.12112735

[84] Helck A, Hummel N, Meinel FG et al. Can single-phase dual-energy CT reliably identify adrenal adenomas? Eur Radiol 2014; 24: 1636–1642. doi:10.1007/s00330-014-3192-z

[85] Mileto A, Nelson RC, Marin D et al. Dual-energy multidetector CT for the characterization of incidental adrenal nodules: Diagnostic performance of contrastenhanced material density analysis. Radiology 2015; 274: 445–454. doi:10.1148/radiol.14140876

[86] Borhani AA, Kulzer M, Iranpour N et al. Comparison of true unenhanced and virtual unenhanced (VUE) attenuation values in abdominopelvic single-source rapid kilovoltage-switching spectral CT. Abdom Radiol 2017; 42: 710–717. doi:10.1007/s00261-016-0991-5

[87] Glazer DI, Maturen KE, Kaza RK et al. Adrenal Incidentaloma Triage With Single-Source (Fast-Kilovoltage Switch) Dual-Energy CT. Am J Roentgenol 2014; 203: 329–335. doi:10.2214/ajr.13.11811

[88] Winkelmann MT, Gassenmaier S, Walter SS et al. Differentiation of adrenal adenomas from adrenal metastases in single-phased staging dual-energy CT and radiomics. Diagnostic Interv Radiol 2022; 28: 208–216. doi:10.5152/dir.2022.21691

[89] Nagayama Y, Inoue T, Oda S et al. Adrenal Adenomas versus Metastases: Diagnostic Performance of Dual-Energy Spectral CT Virtual Noncontrast Imaging and Iodine Maps. Radiology 2020; 296: 324–332. doi:10.1148/radiol.2020192227

[90] Cao J, Lennartz S, Parakh A et al. Dual-layer dual-energy CT for characterization of adrenal nodules: can virtual unenhanced images replace true unenhanced acquisitions? Abdom Radiol 2021. doi:10.1007/s00261-021-03062-3

[91] Ho LM, Marin D, Neville AM et al. Characterization of Adrenal Nodules With Dual-Energy CT: Can Virtual Unenhanced Attenuation Values Replace True Unenhanced Attenuation Values? Am J Roentgenol 2012; 198: 840–845. doi:10.2214/Am J Roentgenol.11.7316

[92] Shern Liang E, Wastney T, Dobeli K et al. Virtual non-contrast detector-based spectral CT predictably overestimates tissue density for the characterisation of adrenal lesions compared to true non-contrast CT. Abdom Radiol 2022; 47: 2462–2467. doi:10.1007/s00261-022-03528-y

[93] Lennartz S, Pisuchpen N, Parakh A et al. Virtual Unenhanced Images: Qualitative and Quantitative Comparison Between Different Dual-Energy CT Scanners in a Patient and Phantom Study. Invest Radiol 2022; 57: 52–61. doi:10.1097/RLI.0000000000000802

[94] Surov A, Hainz M, Holzhausen HJ et al. Skeletal muscle metastases: Primary tumours, prevalence, and radiological features. Eur Radiol 2010; 20: 649–658. doi:10.1007/s00330-009-1577-1

[95] Lennartz S, Große Hokamp N, Abdullayev N et al. Diagnostic value of spectral reconstructions in detecting incidental skeletal muscle metastases in CT staging examinations. Cancer Imaging 2019; 19. doi:10.1186/s40644-019-0235-3

[96] Uhrig M, Simons D, Bonekamp D et al. Improved detection of melanoma metastases by iodine maps from dual energy CT. Eur J Radiol 2017; 90: 27–33. doi:10.1016/j.ejrad.2017.02.024

[97] Andersen MB, Ebbesen D, Thygesen J et al. Impact of spectral body imaging in patients suspected for occult cancer: a prospective study of 503 patients. Eur Radiol 2020; 30: 5539–5550. doi:10.1007/s00330-020-06878-7

[98] Nagayama Y, Nakaura T, Oda S et al. Dual-layer DECT for multiphasic hepatic CT with 50 percent iodine load: a matched-pair comparison with a 120 kVp protocol. Eur Radiol 2018; 28: 1719–1730. doi:10.1007/s00330-017-5114-3

[99] Lennartz S, Hokamp NG, Zäske C et al. Virtual monoenergetic images preserve diagnostic assessability in contrast media reduced abdominal spectral detector CT. Br J Radiol 2020; 93. doi:10.1259/bjr.20200340

[100] Shuman WP, Chan KT, Busey JM et al. Dual-energy CT Aortography with 50% Reduced Iodine Dose Versus Single-energy CT Aortography with Standard Iodine Dose. Acad Radiol 2016. doi:10.1016/j.acra.2015.12.019

[101] Agrawal MD, Oliveira GR, Kalva SP et al. Prospective comparison of reduced-iodine-dose virtual monochromatic imaging dataset from dual-energy CT angiography with standard-iodine-dose single-energy CT angiography for abdominal aortic aneurysm. Am J Roentgenol 2016; 207: W125–W132. doi:10.2214/Am J Roentgenol.15.15814